Eur Biophys J (2008) 37:455–467
DOI 10.1007/s00249-007-0238-z

ORIGINAL PAPER

A domain peptide of the cardiac ryanodine receptor regulates channel sensitivity to luminal Ca^{2+} via cytoplasmic Ca^{2+} sites

Derek R. Laver · Bonny N. Honen · Graham D. Lamb · Noriaki Ikemoto

Received: 24 July 2007 / Revised: 17 October 2007 / Accepted: 28 October 2007 / Published online: 24 November 2007

Abstract The clustering of cardiac RyR mutations, linked to sudden cardiac death (SCD), into several regions in the amino acid sequence underlies the hypothesis that these mutations interfere with stabilising interactions between different domains of the RyR2. SCD mutations cause increased channel sensitivity to cytoplasmic and luminal Ca^{2+}. A synthetic peptide corresponding to part of the central domain (DPc10:^{2460}G–P^{2495}) was designed to destabilise the interaction of the N-terminal and central domains of wild-type RyR2 and mimic the effects of SCD mutations. With Ca^{2+} as the sole regulating ion, DPc10 caused increased channel activity which could be reversed by removal of the peptide whereas in the presence of ATP DPc10 caused no activation. In support of the domain destablising hypothesis, the corresponding peptide (DPc10-mut) containing the CPVT mutation R2474S did not affect channel activity under any circumstances. DPc10-induced activation was due to a small increase in RyR2 sensitivity to cytoplasmic Ca^{2+} and a large increase in the magnitude of luminal Ca^{2+} activation. The increase in the luminal Ca^{2+} response appeared reliant on the luminal-to-cytoplasmic Ca^{2+} flux in the channel, indicating that luminal Ca^{2+} was activating the RyR2 via its cytoplasmic Ca^{2+} sites. DPc10 had no significant effect on the RyR2 gating associated with luminal Ca^{2+} sensing sites. The results were fitted by the luminal-triggered Ca^{2+} feed-through model and the effects of DPc10 were explained entirely by perturbations in cytoplasmic Ca^{2+}-activation mechanism.

Keywords Sudden cardiac death · Calcium release channels · Cardiac muscle · Calcium stores · Excitation–contraction coupling · Ryanodine receptor · Bilayer

Abbreviations

SCD	Sudden cardiac death
CPVT	Catecholaminergic polymorphic ventricular tachycardia
ARVD2	Arrhythmogenic right ventricular cardiomyopathy type 2
SR	Sarcoplasmic reticulum
RyR	Ryanodine receptor
RyR_2	Cardiac ryanodine receptors
$[Ca^{2+}]_L$	Luminal Ca^{2+} concentration
$[Ca^{2+}]_C$	Cytoplasmic Ca^{2+} concentration
TES	N-tris[Hydroxymethyl]methyl-2-aminoethanesulfonic acid
BAPTA	(1,2-bis(o-aminophenoxy)ethane-N,N,N′, N′- tetraacetic acid ($4K^+$)

Introduction

To date, 70 mutations in RyR2 macromolecular complex have been shown to be involved in at least two types of sudden cardiac death (SCD) (Thomas et al. 2006): catecholaminergic polymorphic ventricular tachycardia

D. R. Laver (✉) · B. N. Honen
School of Biomedical Sciences,
University of Newcastle and Hunter Medical Research Institute,
Callaghan, NSW 2308, Australia
e-mail: Derek.Laver@newcastle.edu.au

N. Ikemoto
Boston Biomedical Research Institute,
Watertown, MA 02472, USA

G. D. Lamb
Department of Zoology, La Trobe University,
Melbourne, VIC 3086, Australia

(CPVT) and arrhythmogenic right ventricular cardiomyopathy type 2 (ARVD2) (Tiso et al. 2001; Marks et al. 2002). Both CPVT and ARVD2 are autosomal-dominantly inherited disorders. CPVT is characterised by adrenergic (exercise) induced ventricular tachycardia with no gross structural disorder of the myocardium and ARVD2 is characterised by progressive degeneration of the right ventricular myocardium and arrhythmias.

It is well known that the excitability of Ca^{2+} release from the SR is greatly enhanced by the free Ca^{2+} concentration within the SR lumen (store load, $[Ca^{2+}]_L$) (Cheng et al. 1996; Bers 2001). Ca^{2+} store load most likely varies within the range of $\sim$0.3–1.0 mM during normal cardiac cycling (Bers 2002b). A range of situations such as ischaemia/reperfusion, stress and exercise can lead to an increase in the store load. Beyond a certain level of store overload, RyRs spontaneously release Ca^{2+}. The job of clearing excess Ca^{2+} from the cytoplasm causes over-stimulation of the Na^+/Ca^{2+} exchanger, generating abnormal inward currents across the surface membrane. This current tends to depolarize the membrane, a phenomenon called "delayed-after-depolarisations" (DADs), which can generate premature ventricular contraction and fatal cardiac arrhythmias (Schlotthauer and Bers 2000; Bers 2002a).

The disease-linked mutations in RyR2 are clustered in three discrete regions [N terminal, central and C terminal; some studies further subdivide the C region into two (George et al. 2006, 2007)]. Recent studies have linked SCD mutations from these domains with increased RyR2 activity in response to store load and increased propensity for store-overload induced Ca^{2+} release (Jiang et al. 2004, 2005) and to increased RyR2 sensitivity to cytoplasmic Ca^{2+} (George et al. 2006). Also, it has been directly shown that a CVPT RyR2 mutation leads to DADs and triggered arrhythmias (Liu et al. 2006).

Our recent studies suggest the hypothesis that the N-terminal and central domains of the RyR are normally in close contact. Close contact stabilises the closed state of the channel whereas unzipping of these domains promotes channel opening. The clustering of ARVD2 and CPVT mutations in the central domain indicates that they might interfere with this interaction to cause domain unzipping and aberrant channel activation (Ikemoto and Yamamoto 2002; McCarthy and Mackrill 2004; Lehnart et al. 2005; Oda et al. 2005; George et al. 2006, 2007). Recent structural evidence obtained using cryo-electron microscopy (Wang et al. 2007) shows that the central and N-terminal domains do indeed lie in close proximity ($\sim$3 nm) though the spatial resolution was insufficient to determine the precise nature of any possible interdomain interaction. Several groups have used synthetic peptides corresponding to a section of one of the interacting domains in mouse RyR2 (domain peptides) to study the mechanisms by which RyR2 mutations perturb their function (Ikemoto and Yamamoto 2002; Yamamoto and Ikemoto 2002; Oda et al. 2005; Yang et al. 2006). The rationale is that a domain peptide corresponding to the central domain binds to the N-terminal domain in competition with the in vivo central domain, resulting in the unzipping of RyR2 domains and subsequent activation of the channel, just as would be expected from the RyR2 mutation itself. The peptide approach has the advantage that functional aberration can be induced acutely and reversibly by application and withdrawal of the appropriate peptide. Thus, even minor aberrations can be detected because the same single channel acts as its own control. A crucial test/verification of the peptide approach is that peptides with the disease mutation should be much less effective at perturbing RyR2 function. This is because a mutation made in the domain peptide would reduce its binding affinity to the N-terminal domain of RyR2 in the same way as the corresponding mutation in RyR2 weakens the interaction between the N-terminal and central domains. This is indeed what we and others have seen (Ikemoto and Yamamoto 2002; Yamamoto and Ikemoto 2002; Oda et al. 2005; Yang et al. 2006). The domain peptide DPc10 corresponds to the ^{2460}G–P^{2495} region of rabbit, mouse, human and dog RyR2 which encompasses the human R2474S CPVT mutation in the central domain. DPc10 has been shown to increase [^{3}H]ryanodine binding to isolated RyRs (Yamamoto and Ikemoto 2002) and to increase the RyR-mediated Ca^{2+} leak from the SR of permeabilised cardiomyocytes (Yang et al. 2006) and the R2474S CPVT mutation in DPc10 abolished these effects. As yet, there has been no direct measurement of the effects of DPc10 on single channel function.

Investigations on isolated RyRs in artificial bilayers found that the activity of RyRs was modulated by $[Ca^{2+}]_L$ (Sitsapesan and Williams 1994a; Herrmann-Frank and Lehmann-Horn 1996; Tripathy and Meissner 1996; Gyorke and Gyorke 1998). However, these findings were interpreted in two quite different ways. The "true luminal" hypothesis attributed luminal regulation to Ca^{2+} sites on the *luminal* side of the RyR2 (Sitsapesan and Williams 1995) whereas the "feed-through" hypothesis proposed that luminal Ca^{2+} permeates the pore and binds to *cytoplasmic* Ca^{2+} sites (Herrmann-Frank and Lehmann-Horn 1996; Tripathy and Meissner 1996; Xu and Meissner 1998). It has been suggested that luminal regulation of RyRs somehow involves Ca^{2+} sensing mechanisms on both the luminal and cytoplasmic sides of the membrane (Sitsapesan and Williams 1997; Gyorke et al. 2002). A recent study of the gating kinetics of isolated RyR2s in lipid bilayers indicates that luminal activation of the RyRs occurs by a process of "luminal triggered Ca^{2+} feed-through" (Fig. 1a) in which both luminal and cytoplasmic Ca^{2+} sites mediate channel activation and where these sites are functionally linked by

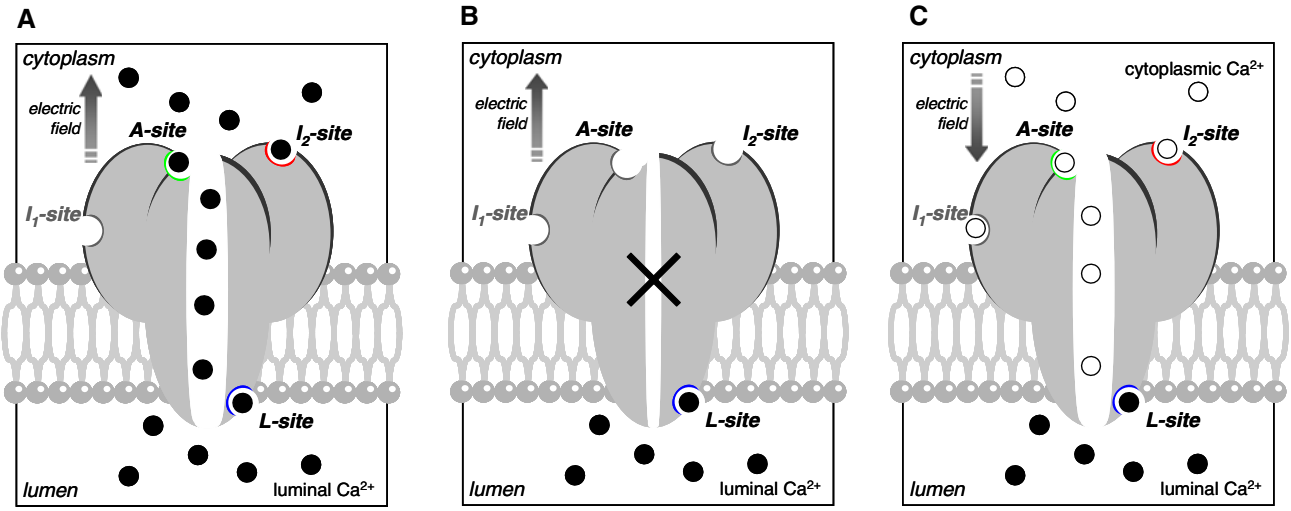

Fig. 1 The process of "luminal triggered Ca^{2+} feed-through" under three experimental conditions. Illustrations of the three Ca^{2+} sensing sites that have been linked to regulation of cardiac RyRs by luminal Ca^{2+}: the luminal activation site (*L*-site, 60 μM affinity), the cytoplasmic activation site (*A*-site, 1–10 μM affinity and the cytoplasmic Ca^{2+}-inactivation site (I_2-site, 1 μM affinity. This site should not be confused with the low affinity (10 mM) Ca^{2+}/Mg^{2+} inhibition site I_1-site, previously referred to as the *I*-site). **a** Cardiac RyR activation by luminal Ca^{2+} (*filled circle*) occurs by a multi-step process in which Ca^{2+} binding to the *L*-site initiates brief (1 ms) openings at rates up to 1 per second. Once the pore is open, luminal Ca^{2+} has access to the *A*-site producing prolongation of openings and to the I_2-site causing inactivation at high levels of Ca^{2+} feed-through. **b** At sub-activating $[Ca^{2+}]_C$ (≤0.1 μM) and during intervals when the channel is shut, the *L*-site is the only trigger for channel opening. Hence, the channel opening rate gives an unambiguous measure of the *L*-site properties. **c** A sufficiently large electrochemical gradient in opposition to Ca^{2+} feed-through (e.g. +40 mV and $[Ca^{2+}]_L \leq 100$ μM) can effectively prevent luminal Ca^{2+} from binding to the cytoplasmic sites. Under these conditions it is possible to unambiguously measure the effects of cytoplasmic Ca^{2+} (*open circle*) on the *A*- and I_2-sites

the flow of Ca^{2+} through the pore (Ca^{2+} feed-through) (Laver 2007).

The fact that RyR2 activation by luminal and cytoplasmic Ca^{2+} share common modes of action (Fig. 1a) means that *any* cofactor that prolongs channel openings triggered by $[Ca^{2+}]_C$ should also promote RyR2 activation by $[Ca^{2+}]_L$ via Ca^{2+} feed-through, as has been demonstrated for the case of ATP (Laver 2007). Here, we also demonstrate this for DPc10 and draw comparisons between the actions of these two RyR2 agonists. By controlling the magnitude of Ca^{2+} feed-through via membrane voltage (c.f. Fig .1a, c), this study aims to determine how the luminal and cytoplasmic sites are affected by DPc10 in the absence and presence of Ca^{2+} feed-through and to infer how SCD mutations might lead to mal-regulation by store load of RyR2s. This is the first investigation of how DPc10 alters the regulation of RyR2 activity by luminal Ca^{2+}.

Materials and methods

Solutions

Sarcoplasmic reticulum vesicles (containing RyR2) were obtained from sheep hearts and were reconstituted into artificial lipid bilayers as previously described (Laver et al. 1995). Lipid bilayers were formed from phosphatidylethanolamine and phosphatidylcholine (8:2 wt/wt) in *n*-decane, (50 mg/ml). During experiments the *cis* (cytoplasmic) and *trans* (luminal) solutions contained 250 mM Cs^+ (230 mM $CsCH_3O_3S$, 20 mM CsCl) and various concentrations of $CaCl_2$. The composition of the *cis* solution was altered either by aliquot addition of stock solutions or by local perfusion which allowed solution exchange within ~1 s (Laver and Lamb 1998; O'Neill et al. 2003). The *trans* solution was altered by aliquot addition.

Solutions were pH buffered with 10 mM TES and solutions were titrated to pH 7.4 using CsOH. Free $[Ca^{2+}]$ up to 100 nM was estimated using published association constants (Marks and Maxfield 1991) and the program "Bound and Determined" (Brooks and Storey 1992) and concentrations higher than this were measured using a Ca^{2+} electrode (Radiometer). $[Ca^{2+}]$ below 10 μM was buffered with 4.5 mM BAPTA and titrated with $CaCl_2$· $[Ca^{2+}]$ in the range 10–50 μM was buffered with sodium citrate (up to 6 mM).

The peptides DPc10 (^{2460}GFCPDHKAAMVLFLD**R**VY GIEVQDFLLHLLEVGFLP^{2495}) and DPc10-mut containing the R2474S mutation (^{2460}FCPDHKAAMVLFLD**S**VY GIEVQDFLL HLLEVGFLP ^{2495}) were synthesised on an applied Biosystems model 431A synthesiser employing Fmoc (N-(9-fluorenly) methoxycarbonyl) as the amino protecting group. Peptides were cleaved and de-protected

with 95% trifluoroacetic acid and purified by reverse phase high-pressure liquid chromatography.

Acquisition and analysis of ion channel recordings

Bilayer apparatus and data recording methods are described elsewhere (Laver et al. 2004). Electrical potentials are expressed using standard physiological convention (i.e. cytoplasmic side relative to the luminal side at virtual ground). Measurements were carried out at 23 ± 2°C. Prior to analysis the current signal was digitally filtered at 1 kHz with a Gaussian filter and sampled at 5 kHz. Single channel properties were measured using Channel2 software. Open probability (P_o) and mean open and closed durations (τ_o and τ_c) were calculated from single channel records using a threshold discriminator at 50% of channel amplitude. Ca^{2+}-dependencies of channel open probability, τ_o and opening rate ($1/\tau_c$) were characterised by fitting these data with Hill curves using the following equations for activation and inactivation (shown here for the case of P_o, similar equations apply to τ_o and opening rate):

$$P_o = P_{min} + \frac{(P_{max} - P_{min})\left([Ca^{2+}]/K_a\right)^{n_a}}{1 + \left([Ca^{2+}]/K_a\right)^{n_a}}$$

$$P_o = P_{min} + \frac{(P_{max} - P_{min})}{1 + \left([Ca^{2+}]/K_i\right)^{n_i}}$$

P_{min} and P_{max} are the activities of the minimally and maximally activated channel, K_a and K_i are the $[Ca^{2+}]$ for half activation and inhibition, and n_a and n_i are the corresponding Hill coefficients.

Statistics

Data points are displayed as means ± standard error on the mean. Significance was calculated using either the Binomial test for less than ten samples or the Sign test for larger numbers of samples. The theory was fitted with the data using the method of least squares. Details of the development of the luminal-triggered Ca^{2+} feed-through model, its kinetic schemes and equations, and the methods for generating model predictions are given in (Laver 2007).

Results

Effect of DPc10 on RyR2 activity

Figure 2 shows the effect of DPc10 on a single sheep cardiac RyR in a lipid bilayer at −40 mV. In this case the channel was activated under control conditions by 3 μM Ca^{2+} in the cytoplasmic bath. DPc10 (100 μM) was rapidly applied to the cytoplasmic side of the channel by bath

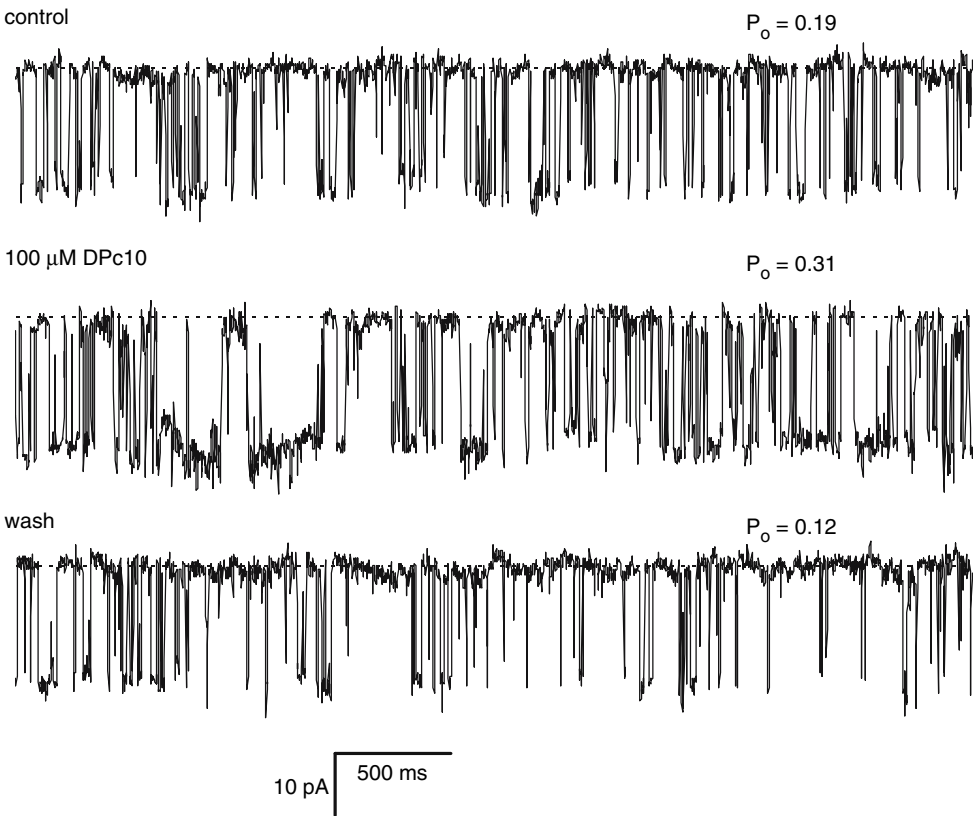

Fig. 2 DPc10 reversibly activates RyR_2. Representative traces showing the effect of 100 μM DPc10 (cytoplasmic) on a cardiac RyR in a bilayer. The addition of DPc10 activated the RyR2 and subsequent removal of DPc10 by bath perfusion (wash) returned channel activity to control levels. The $[Ca^{2+}]$ in the cytoplasmic and luminal baths were 3 and 100 μM, respectively. The traces were taken from a single experiment and the channel open probability for the entire record P_o, is shown at the right of each trace. Channel openings are downward current jumps from the baseline (*dashed lines*) where the channels are closed

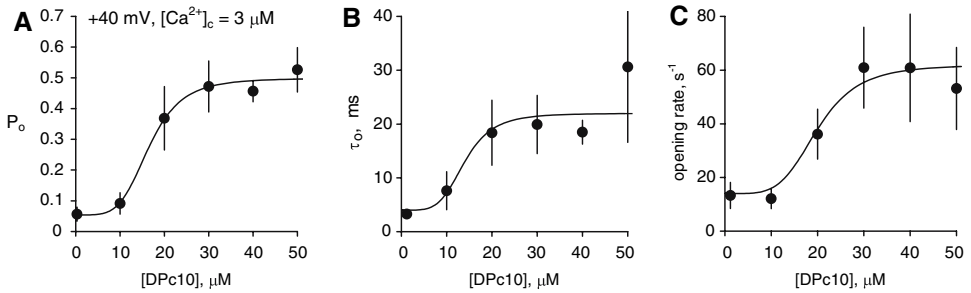

Fig. 3 DPc10 Concentration dependencies of P_o **a** mean open time **b** and opening rate **c**. The $[Ca^{2+}]$ in the cytoplasmic and luminal baths were 3 and 100 μM, respectively and the bilayer voltage = +40 mV. The *solid curves* shows Hill fits to the data with Hill coefficients = 4 and K_as = 17 μM for P_o, 14 μM for mean open time and 20 μM for opening rate. The data points show the mean ± SEM of 4–6 measurements

perfusion (see Materials and methods). This caused a marked increase in channel activity within 15–30 s of application. The effect could be reversed by perfusion of the bath with the same solution without peptide. The reversibility of DPc10 activation was measured in 15 experiments in which peptide application increased activity by a mean factor of 3 ± 1. After washout of the peptide the channel activities returned to 104 ± 20% of their respective control levels.

Figure 3 shows the DPc10 concentration dependence of RyR2 activation measured in the presence of 3 μM cytoplasmic Ca^{2+} ($[Ca^{2+}]_C$) and 100 μM luminal Ca^{2+} ($[Ca^{2+}]_L$) at +40 mV. RyR2 open probability (P_o) had a sigmoidal dependence on [DPc10] with an K_a of 17 μM and a Hill coefficient of 4 (Fig. 3a). The Hill coefficient indicates that a large fraction of the activation requires binding at four peptide binding sites on the RyR (probably one per subunit of the homotetramer). Activation of the channels was associated with increases in both the mean open time (τ_o, Fig. 3b) and opening rate ($1/\tau_c$, Fig. 3c) that each had similar K_as of 14 and 20 μM, respectively. This suggests that peptide binding is not dependent on the channels open state.

The results of paired experiments show that DPc10 activated RyRs in the presence of 1 mM $[Ca^{2+}]_L$ at +40 mV (Fig. 4). DPc10 (100 μM, filled circle) produced a significant (asterisks) 2–4 fold increase in P_o with the largest relative effects occurring at low $[Ca^{2+}]_C$ (≤0.1 μM). The results are displayed as relative potentiating effects of DPc10 on P_o derived from paired measurements with and without DPc10 in the same channel, as this obviated problems with channel-to-channel variability and allowed us to identify even small changes in channel properties. DPc10-mut produced no significant increase in P_o at +40 mV (100 μM, Fig. 4, open square) nor at −40 mV (1.0 ± 0.7-fold, $n = 4$, $[Ca^{2+}]_C = 0.3$ μM and $[Ca^{2+}]_L$ = 0.1 mM). An important negative control for testing the effects of DPc10 on domain zipping in RyR2 is that the activating effect of DPc10 should be abolished by the *R*-to-*S* substitution (DPc10-mut) corresponding to the R2474S; the SCD-linked mutation in RyR2. Figure 4 shows this indeed to be the case suggesting that DPc10 activation occurs via a process of domain destabilisation.

Effects of DPc10 on RyR2 regulation by $[Ca^{2+}]_C$

In the following experiments, the $[Ca^{2+}]_C$-dependence of DPc10 activation was measured using 100 μM $[Ca^{2+}]_L$ because, at this $[Ca^{2+}]_L$, the effects of Ca^{2+} feed-through can be enhanced or inhibited simply by switching the voltage between ±40 mV [(Laver 2007), also compare Fig. 1a, c)]. Paired measurements of P_o, τ_o and opening

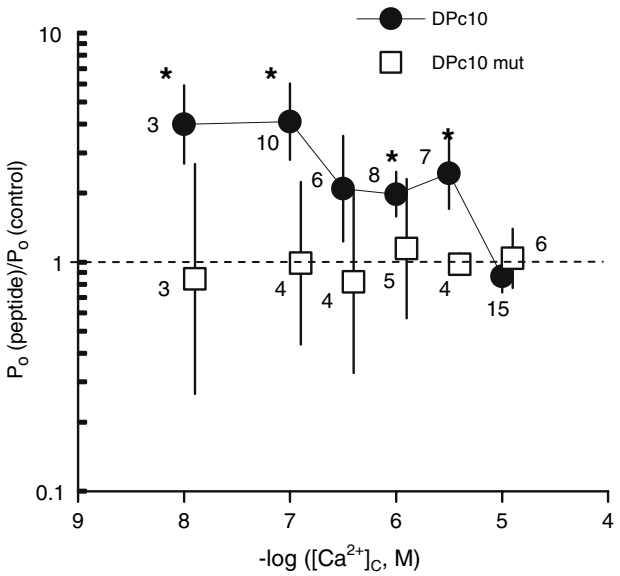

Fig. 4 The effect of cardiac domain peptides on P_o of RyR_2 at various $[Ca^{2+}]_C$ (+40 mV, $[Ca^{2+}]_L$ = 1 mM). The effects of DPc10 (*filled circle*) and DPc10-mut containing the R2474S mutation (*open square*) were normalized to P_o measured under control conditions in the same channels. *Data labels* indicate the number of replicates and the *asterisks* indicate significant changes in activation ($P < 0.05$)

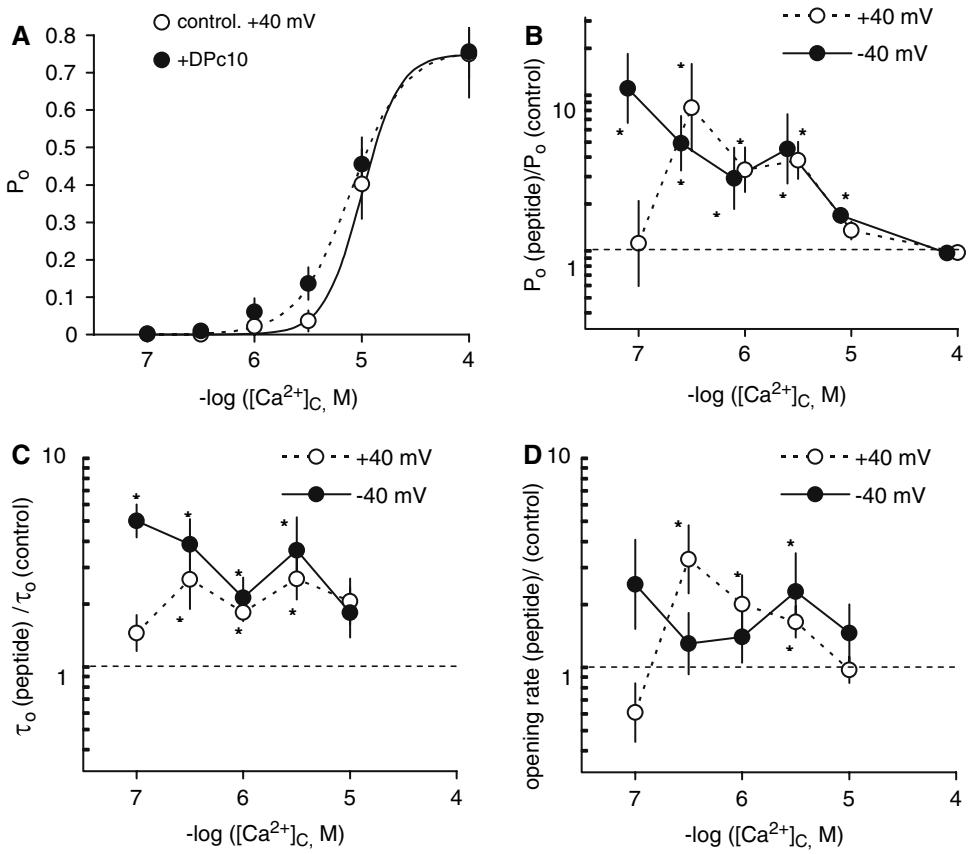

Fig. 5 The effect of $[Ca^{2+}]_C$ and DPc10 on paired measurements of P_o (**a**, **b**), mean open time (τ_o) **c** and opening rate ($1/\tau_c$) **b**. **a** The open probability of RyRs in the presence of 100 μM DPc10 (*filled circle*) and in its absence (*open circle*) (+40 mV). The data points show mean ± SEM of 4–11 paired measurements. (*solid*/control) K_a = 10 ± 1.6 μM, P_{max} = 0.74 ± 0.08, n_a = 2.5 ± 1.5 and (*dashed*/DPc10) K_a = 5 ± 1.3 μM, P_{max} = 0.76 ± 0.09, n_a = 2.0 ± 1.0. (*filled circle*) in the presence of 100 μM DPc10 and (*open circle*) in its absence. **b–d** The effects of DPc10 normalized to control conditions in the same channels at −40 mV (*filled circle*) and +40 mV (*open circle*). Experimental conditions were $[Ca^{2+}]_L$ = 100 μM and the indicated $[Ca^{2+}]_C$. Data points show mean ± SEM of *n* paired measurements. *open circle* (from low to high $[Ca^{2+}]_C$) *n* = 4, 6, 10, 11, 6, 3; *filled circle n* = 6, 6, 9, 9, 6, 3). *Asterisks* in **b–d** indicate significant changes in activation ($P < 0.05$)

rate at +40 mV (i.e. in the virtual absence of Ca^{2+} feed-through), reveal that the $[Ca^{2+}]_C$-activation characteristics of RyR2 are altered by DPc10 (Fig. 5). DPc10 reduces K_a from 10 to 5 μM (Fig. 5a, $P < 0.01$). At +40 mV, relative DPc10 activation displays a maximum between 0.3 and 1 μM $[Ca^{2+}]_C$ (Fig. 5b, open circle) which is associated with significant, 2–3 fold increases in both τ_o (Fig. 5c) and opening rate (Fig. 5d). At −40 mV the activation by DPc10 is similar to that at +40 mV except at 0.1 μM $[Ca^{2+}]_C$ where DPc10 activation is considerably enhanced (presumably by Ca^{2+} feed-through; see below).

Figure 6 shows the $[Ca^{2+}]_C$-dependencies of τ_o and opening frequency and the effects of DPc10 and of ATP (ATP effects are described below). At +40 mV (Fig. 6a, b, again, in the absence of Ca^{2+} feed-through), increasing $[Ca^{2+}]_C$ in the absence of DPc10 (open circle) caused a large increase in opening rate but had very little effect on τ_o. DPc10 (filled circle) increased τ_o at $[Ca^{2+}]_C > 0.1$ μM and caused a small increase in opening rate. At −40 mV, where Ca^{2+} feed-through is favoured (Fig. 6c, d), the effects of $[Ca^{2+}]_C$ and DPc10 on opening rate were similar to those described for +40 mV. DPc10 produced similar increases in τ_o at ±40 mV when $[Ca^{2+}]_C$ = 10 μM (∼twofold; note different ordinate scales in Panels A and C in Fig. 6). However, at lower $[Ca^{2+}]_C$ (0.1–0.3 μM) DPc10 produced a much larger increase in τ_o at −40 mV than at +40 mV (∼5–7 fold). Thus it appears that DPc10 has some activating effects that are not associated with Ca^{2+} feed-through (voltage-independent increase in τ_o) and more conspicuous activating effects that rely on Ca^{2+} feed-through (voltage-dependent increase in τ_o, which was particularly apparent at low $[Ca^{2+}]_C$, ∼0.1–0.3 μM). A more precise interpretation of these data within the framework of the luminal-triggered Ca^{2+} feed-through model is given below.

ATP is a strong activator of RyR2 which shifted the K_a for cytoplasmic Ca^{2+} activation from 10 to 1 μM (Laver 2007). Data showing the effects of ATP on

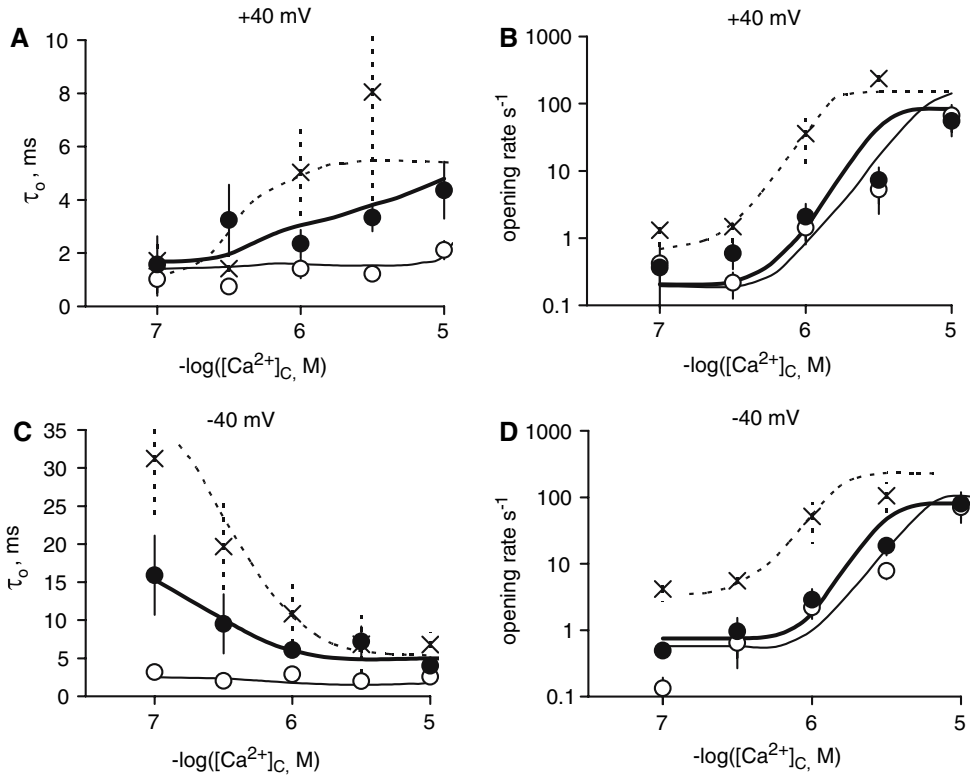

Fig. 6 RyR2 activation by "luminal triggered Ca^{2+} feed-through" and the effects of DPc10 or ATP. **a**, **c** Mean open times **b**, **d** mean opening rate in the presence of 100 μM DPc10 (*filled circle*), 2 mM cytoplasmic ATP (x) and in their absence (*open circle*). Control and DPc10 data shows the mean ± SEM of 4–11 paired measurements. The ATP data is taken from (Laver 2007). Experimental conditions were $[Ca^{2+}]_L$ = 100 μM and the indicated $[Ca^{2+}]_C$. Under these experimental conditions, at −40 mV the membrane potential favours Ca^{2+} flow from lumen to cytoplasm while at +40 mV it opposes Ca^{2+} flow (see Fig. 1). DPc10 increased the channel open durations at −40 mV. The lines show fits of the luminal triggered Ca^{2+} feed-through model to data obtained from RyRs under control conditions (*thin*), in the presence of DPc10 (*thick*) or ATP (*dashes*). The parameter values for three experimental conditions are given in Table 1

channel kinetics, taken from Laver (2007), are compared with the effects of DPc10 in Fig. 6. ATP had a much larger effect on RyR2 activity than DPc10. ATP caused a 40-fold increase in the channel opening rate (Fig. 6b, d; ×) and an increase in the duration of channel openings that was ∼twofold larger that achieved by DPc10 (Fig. 6a, c; ×).

Effects of $[Ca^{2+}]_L$ and voltage (Ca^{2+} feed-through) on DPc10 activation

To explore the possible role of luminal Ca^{2+} and Ca^{2+} feed-through on DPc10 activation we measured RyR2 activity over a range of $[Ca^{2+}]_L$ in the presence of 0.1 μM $[Ca^{2+}]_C$ at ±40 mV. Figure 7 shows the $[Ca^{2+}]_L$-dependence of P_o, τ_o and opening rate of RyRs in the presence DPc10 compared with that of a different group of channels in the absence of DPc10. At −40 mV, in the absence of peptide (open circle), increasing $[Ca^{2+}]_L$ increased P_o to a maximum of 0.003 (Fig. 7a). τ_o did not depend strongly on $[Ca^{2+}]_L$ (Fig. 7b) whereas the opening rate exhibited a hyperbolic dependence on $[Ca^{2+}]_L$ (Fig. 7c) indicative of Ca^{2+}-activation via the *L*-site (see Fig. 1b) with a K_L of 35 ± 8 μM and a maximal opening rate of 1.17 ± 0.09 per second.

In the presence of 100 μM DPc10 (filled circle) P_o was ∼threefold higher than in its absence (Fig. 7a). It did this via a substantial change to the $[Ca^{2+}]_L$-dependence of τ_o with no significant change to opening rate ($P > 0.1$ using the *t* test; Fig. 7b, c). In the presence of DPc10 τ_o had a strongly peaked, bell-shaped dependence on $[Ca^{2+}]_L$ in which τ_o increased with $[Ca^{2+}]_L$ between 10 and 50 μM and declined at higher $[Ca^{2+}]_L$. The $[Ca^{2+}]_L$—dependence of opening rate had a K_L = 27 ± 5 μM with a maximal opening rate of 1.2 ± 0.3 per second (Fig. 7c). These parameters were not significantly different from those obtained in the absence of DPc10 (see above). In a series of paired experiments, DPc10 caused no significant increase in opening rate but did produce a significant increase in τ_o over the $[Ca^{2+}]_L$ range 10–100 μM (Fig. 7d).

At positive voltage (+40 mV) which opposes Ca^{2+} feed-through, the $[Ca^{2+}]_L$-dependence of DPc10-activation was shifted to higher $[Ca^{2+}]_L$, producing activation of RyRs

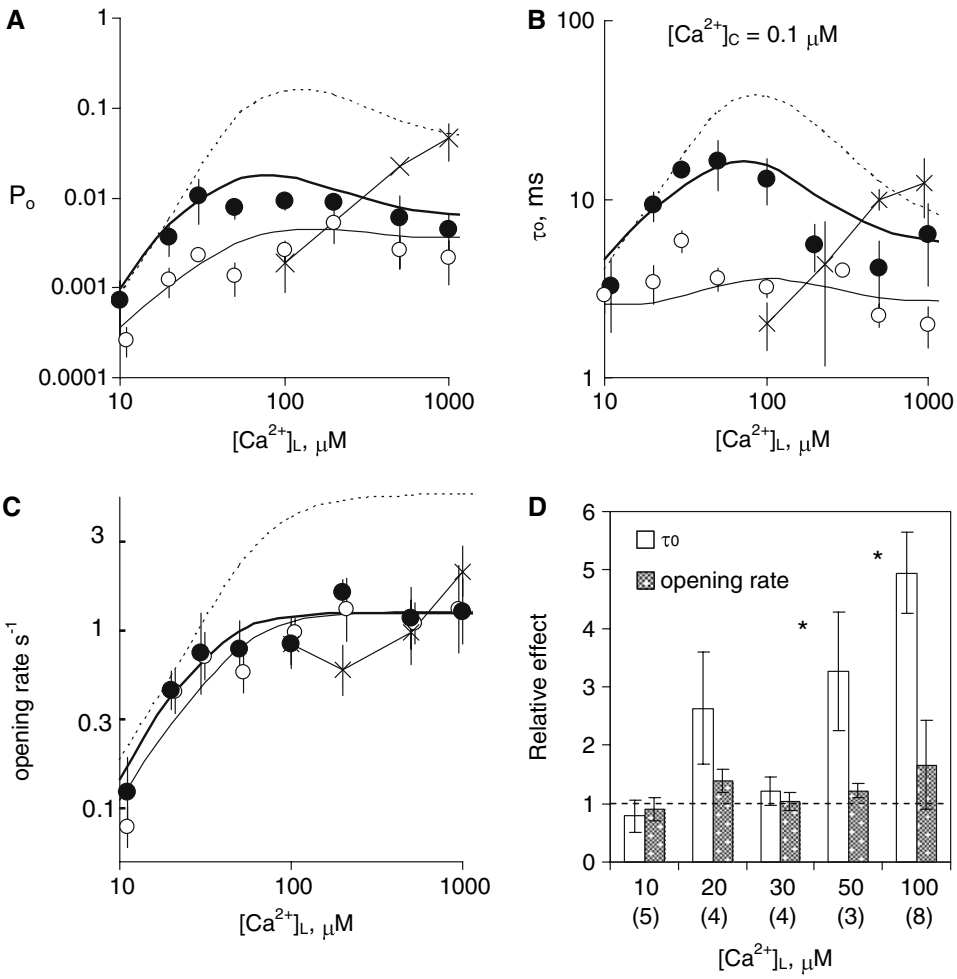

Fig. 7 The effect of $[Ca^{2+}]_L$ and DPc10 on P_o **a** mean open times, **b** and mean opening rate **c**. In all experiments $[Ca^{2+}]_C$ = 0.1 μM. (*filled circle*) 100 μM DPc10, −40 mV, n = 3–8; (*open circle*) control, −40 mV, n = 3–14; (x) 100 μM DPc10, +40 mV, n = 4–9. The *lines* show fits of the luminal triggered Ca^{2+} feed-through model to data obtained from RyRs under control conditions (*thin*), in the presence of DPc10 (*thick*) or ATP (*dashes*, ATP data not shown). The parameter values for three experimental conditions are given in Table 1. **d** The effect of $[Ca^{2+}]_L$ and DPc10 on paired measurements of τ_o and opening rate. The number of experiments are indicated in *parentheses* and *asterisks* indicate significant changes in activation ($P < 0.05$)

over the $[Ca^{2+}]_L$ range 100–1000 μM (Fig. 7, ×), and produced no change in the mean opening rate. These results demonstrate that at −40 mV, DPc10 has its maximal activating effect on RyRs at 100 μM $[Ca^{2+}]_L$, whereas at +40 mV this $[Ca^{2+}]_L$ is sub-activating.

ATP had a much larger effect than DPc10 on RyR2 response to $[Ca^{2+}]_L$ (Fig. 7, dashed line; from Laver 2007). ATP caused 30-fold increase in responses of P_o and τ_o to $[Ca^{2+}]_L$ but had no significant effect on K_L (60 ± 20 μM vs. 35 ± 5 μM in the absence of ATP). The effect of DPc10 was investigated in the presence of 2 mM ATP at 0.1 μM $[Ca^{2+}]_C$. When DPc10 was applied to RyRs in the presence of ATP there was no discernible increase in channel activity. Figure 8 shows the relative changes in P_o, τ_o and opening rate induced by DPc10 in the presence of 2 mM ATP, 0.1 μM $[Ca^{2+}]_C$ at three $[Ca^{2+}]_L$ representing sub-activating (0 μM, ±40 mV), maximally activating (100 μM, −40 mV) and inactivating concentrations (1 mM, −40 mV). Under all experimental conditions DPc10 had no significant effect on channel gating kinetics.

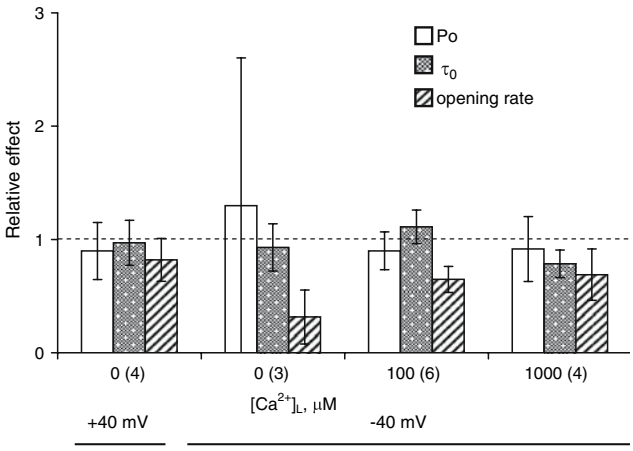

Fig. 8 The effect of DPc10 on RyR2 kinetics in the presence of 2 mM ATP. The effects of DPc10 at two membrane voltages are normalized to control conditions in the same channels. The data shown in the four groupings on the *left* were obtained from RyRs in the presence of $[Ca^{2+}]_C$ = 0.1 μM and the indicated $[Ca^{2+}]_L$. The number of experiments for each condition are given in *parentheses*

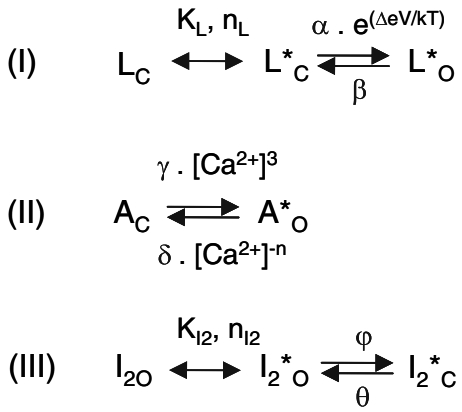

Fig. 9 Kinetic schemes for Ca^{2+} binding at the *L*-, *A*- and I_2-sites (Schemes I–III, respectively). Together these sites regulate RyR2 activity as follows: RyR2 opening can be triggered by activation of either the *A*- or *L*-sites but Ca^{2+} binding to the I_2-site is sufficient to close the channel. *Asterisks* indicate sites occupied with Ca^{2+}. The open and closed status of the channel associated with each kinetic state is indicated by the subscripts "O" and "C", respectively. In Schemes I and III the Ca^{2+} binding/unbinding steps are thought to be fast compared to the gating of the channel and these steps are characterised by their Ca^{2+} affinities, $K_{L,I2}$ and Hill coefficients, $n_{L,I2}$. Scheme II is a representation of complex multi-step process (Zahradnik et al. 2005). Hence the reaction rates have complex dependencies on $[Ca^{2+}]$. The parameter, *n*, in Scheme II accounts for the $[Ca^{2+}]_C$-dependent increase in channel mean open times caused by ATP and DPc10. The full set of equations for the transition reaction rates are given in Table 1 of (Laver 2007) and the parameter values for various experimental conditions are given in Table 1 here

The effect of DPc10 on luminal-triggered Ca^{2+} feed-through

Evidence suggests that RyR2 regulation by luminal Ca^{2+} is mediated by one class of luminal Ca^{2+} site (*L*-site) and two classes of cytoplasmic Ca^{2+} sites (*A*- and I_2-sites, Fig. 1). Kinetic schemes describing the action of Ca^{2+} at these sites are given in Fig. 9. The RyR2 can be opened by Ca^{2+} binding to either the *A*-site or the *L*-site whereas Ca^{2+} binding to the I_2-site closes the channel (Fig. 9). In the virtual absence of cytoplasmic Ca^{2+}, as is the case during cardiac diastole, the binding of Ca^{2+} to the *L*-site on its own can activate channel openings of $\sim$1 ms duration at rates up to 1 per second. Once the channel is open, the flux of Ca^{2+} from the luminal to cytoplasmic sides of the channel (Ca^{2+} feed-through) increases $[Ca^{2+}]_C$ in the vicinity of the *A*-site and substantially prolongs channel openings. In addition, the I_2-site causes a reduction in channel open durations at high levels of Ca^{2+} feed-through.

This section gives an account of the data within the framework of the model starting with the data obtained from experiments where the complicating effects of Ca^{2+} feed-through are either small (Fig. 6a where the voltage opposes Ca^{2+} feed-through, also see Fig. 1c) or non existent (Fig. 6b, d; opening rate is a property of the closed state of the channel where there is no Ca^{2+}-feed through, also see Fig. 1b). The model accounts for the $[Ca^{2+}]_C$-dependence of RyR2 opening rate in the absence of peptide (Fig. 6b, d; thin curve) in three-phases. In the virtual absence of cytoplasmic Ca^{2+} ($\leq$0.3 μM) the opening rate is governed by the openings triggered by the binding of luminal Ca^{2+} to the *L*-site (phase 1). At higher $[Ca^{2+}]_C$, opening rate increases ($\propto[Ca^{2+}]_C^3$) due to openings triggered by the binding of cytoplasmic Ca^{2+} to the *A*-site (phase 2). When $[Ca^{2+}]_C$ reaches 10 μM the concentration dependence plateaus because the channel opening rate becomes limited by the I_2 reactivation step (θ in Scheme III, phase 3). Therefore, the DPc10-induced increase in channel opening rate which occurs for $[Ca^{2+}]_C$ = 0.3–3 μM (phase 2) but not outside this range (Fig. 6b, d, thick curve) can be explained by a twofold increase in the opening rate associated with the *A*-site (see Table 1, γ).

The mean open time of the RyR2 in the absence of peptide (Fig. 6a, thin curve) is dominated by the closing rate associated with the *A*-site which is insensitive to $[Ca^{2+}]_C$ (i.e. $n = 0$ in Scheme II). The DPc10 induced increase in τ_o (Fig. 6a, thick curve) can be explained by a Ca^{2+}-dependent decrease in closing rate (i.e. $\propto [Ca^{2+}]_C^{-1}$, $n = 1$ in Scheme II). The effects of this are tempered by the increased closing rate associated with the I_2-mediated inactivation mechanism.

The dependence of opening rate on $[Ca^{2+}]_L$, at sub-activating $[Ca^{2+}]_C$ (Fig. 7c), depends solely on the properties of Scheme I. The EC_{50} for the channel opening rate is determined by K_L while the maximal channel opening rate is determined by $\alpha \times \exp(\Delta eV/kT)$. The model fit indicated that DPc10 had no significant effect on K_L or maximal rate of luminal triggered openings, α. Thus, we could find no indication that the activating effect of DPc10 was in any way due to alterations in the *L*-site.

When experimental conditions favour Ca^{2+} feed-through (−40 mV; Figs. 6c, 7a, b), Ca^{2+} emanating from the pore will diffuse into the cytoplasm and be sequestered by buffering molecules, leading to a decline in $[Ca^{2+}]$ with radial distance from the pore (Stern 1992). Therefore Ca^{2+} sites that are further away from the pore will be less sensitive to the effects of Ca^{2+} feed-through than sites near the pore. The magnitude of Ca^{2+} feed-through and the model parameters associated with Ca^{2+} feed-through (*X* and *Y*, see Table 1) have been determined previously (Laver 2007) and the same parameter values are used in this study. The potentiating effect of DPc10 on $[Ca^{2+}]_L$-dependent activation (Fig. 7a, b) can be modelled primarily by Ca^{2+} feed-through coupled with the effect of DPc10 on the closing rate associated with the *A*-site (i.e. τ_o). The decline τ_o seen with increasing $[Ca^{2+}]_C$ (Fig. 6c) can be explained by the effects of cytoplasmic Ca^{2+} on the I_2-site whereas the decline τ_o seen with increasing $[Ca^{2+}]_L$ greater than

Table 1 Parameters of the "luminal-triggered Ca^{2+} feed-through" model

Ca^{2+} site	Parameter	Symbol	Control	DPc10 100 μM	ATP 2 mM
L-site	Affinity, Hill constant	K_L, n_L	35 μM, 2	27 μM, 2	60 μM, 2
♣*	Opening rate (0 mV)	α	1.0 s^{-1}	1.0 s^{-1}	2.7 s^{-1}
	V-dependence	Δ	0.4	0.4	0.4
	Closing rate	β	1,000 s^{-1}	1,000 s^{-1}	1000 s^{-1}
A-site +♣*	Affinity, Hill constant	K_A, n_A	10 μM, 2.5	5 μM, 2	1 μM, 2
+♣*	Opening rate	γ	2.0 s^{-1} μM^{-3}	4.0 s^{-1} μM^{-3}	43 s^{-1} μM^{-3}
+♣*	Closing rate	δ	700 s^{-1}	350 s^{-1} μM	220 s^{-1} μM
+♣*	Ca^{2+}-dependence	n	0	1	1
	Ca^{2+} feed-through	X	15 μM/pA	15 μM/pA	15 μM/pA
I_2-site ♣*	Affinity, Hill constant	K_{I2}, n_{I2}	0.8 μM, 2	0.8 μM, 2	1.5 μM, 2
	Opening rate	θ	100 s^{-1}	100 s^{-1}	200 s^{-1}
	Closing rate	φ	250 s^{-1}	250 s^{-1}	250 s^{-1}
	Ca^{2+} feed-through	Y	0.35 μM/pA	0.35 μM/pA	0.35 μM/pA

The model was fitted to RyR2 kinetic data obtained in the presence and absence of DPc10 and ATP. A description of opening and closing rates associated with each site is given in Fig. 8. K_A and n_A are derived from Hill fits to the $[Ca^{2+}]_C$-dependencies of P_o in Fig. 5a and were not used in the fitting of the model. + Indicates a significant effect of DPc10, ♣ a significant effect of ATP and * indicates a significant difference between the effects of DPc10 and ATP ($P < 0.05$). Model fits are shown in Figs. 6 and 7

100 μM (Fig. 7b) can be explained by the effects Ca^{2+} feed-through on the I_2-site. Interestingly, the model predicts that luminal Ca^{2+} will have a substantially larger effect than cytoplasmic Ca^{2+} on τ_o. This is because the *A*- and I_2-sites have similar sensitivity to cytoplasmic Ca^{2+} so that $[Ca^{2+}]_C$-activation and inhibition effects tend to cancel. However, the I_2-site is less sensitive to the effects of Ca^{2+} feed-through than the *A*-site because the I_2-site is further from the pore (see above), resulting in a net gain in RyR2 activation by $[Ca^{2+}]_L$. In summary, the effects of DPc10 on the regulation of RyR2 by cytoplasmic and luminal Ca^{2+} could be explained entirely by a perturbation of channel gating associated with the *A*-site (Table 1, +). This is quite different to ATP which had activating effects via all three Ca^{2+} sensing mechanisms. It increased the *L*-site mediated opening rate, increased τ_o in response to Ca^{2+} binding at the *A*-site and decreased the rate of inactivation via the I_2-site (Table 1, ♣).

Discussion

The effects of DPc10 and DPc10-mut on activation of single RyR2 channels observed here match well with the findings obtained from [^{3}H]ryanodine binding measurements (Yamamoto and Ikemoto 2002). Both assays of RyR2 activity show that DPc10 slightly increased the sensitivity of RyRs to cytoplasmic Ca^{2+} (Fig. 5a). Furthermore, they show a very similar dependence of DPc10 activation on cytoplasmic Ca^{2+} in that the relative effects of DPc10 activation is greatest at ~0.3 μM Ca^{2+} [compare Fig. 2 in (Yamamoto and Ikemoto 2002)]. The total lack of effect of DPc10-mut on single channel activity supports the hypothesis that both DPc10 and the R2474S mutation in RyR2 prevent domain–domain interactions. These effects of DPc10 and DPc10-mut in single channel and [^{3}H]ryanodine binding assays also tally with the peptide-induced increase in cytoplasmic Ca^{2+} sensitivity of Ca^{2+} release in permeabilised cardiomyocytes (Yang et al. 2006). In addition, this study demonstrates that the activating effect of DPc10 is readily reversible and depends on luminal Ca^{2+} and membrane potential. The fact the DPc10 activation is reversed by washout rules out the possibility that DPc10 acts by dissociating an important accessory protein such as FKBP12.6.

Besides the effect of increasing the sensitivity of the channel to the cytoplasmic Ca^{2+} described above, we found substantial activation by DPc10 that can be attributed to Ca^{2+} feed-through. In the presence of sub-activating $[Ca^{2+}]_C$, DPc10 activation can be prevented by reduced $[Ca^{2+}]_L$ or by positive membrane potentials that inhibit the feed-through of luminal Ca^{2+}. This is seen in Fig. 7b where the DPc10-induced increase in open times is substantially enhanced when $[Ca^{2+}]_L$ is raised from 10 to 100 μM. However, positive membrane potentials (+40 mV) that oppose Ca^{2+} feed-through eliminated DPc10 activation at 100 μM and shifted its activation to 1 mM luminal Ca^{2+}.

By fitting the luminal-triggered Ca^{2+} feed-through model to the data in Figs. 6 and 7 we show that the effects of DPc10 on cytoplasmic and luminal Ca^{2+} regulation of RyR2 could be explained entirely by perturbations of channel gating associated with the *A*-site. Moreover, we explain the potentiating effect of DPc10 on $[Ca^{2+}]_L$ activation by Ca^{2+} feed-through which links cytoplasmic and

luminal Ca^{2+} regulation of RyR2. In fact, according to this model, any cofactor or channel aberration/mutation that prolongs channel openings induced by cytoplasmic Ca^{2+} will also promote RyR2 activation by luminal Ca^{2+} feed-through. $[Ca^{2+}]_L$-dependent activation of RyRs is known to be increased by enhancers of $[Ca^{2+}]_C$-activation (Sitsapesan and Williams 1994b; Lukyanenko et al. 1996; Gyorke and Gyorke 1998). The effects of ATP have already been interpreted within the framework of the "luminal triggered Ca^{2+} feed-through" model (Laver 2007) and here we compare the effects of DPc10 with those of ATP (Figs. 6, ×, 7, dashed curves). Although ATP and DPc10 are both activators of RyR2, they appear to have quite different effects on channel kinetics. DPc10 caused smaller increases in τ_o and opening rate than did ATP. The model reveals the different actions of ATP and DPc10 on the gating mechanisms associated with the *A*-, *L*- and I_2-sites. ATP had activating effects via all three mechanisms. It increased the *L*-site mediated opening rate, increased τ_o in response to Ca^{2+} binding at the *A*-site and decreased the rate of inactivation via the I_2-site (Table 1, ♣). On the other hand, DPc10 had more specific effects on the RyR, only perturbing the *A*-site (Table 1, +), and doing so to a lesser much extent than ATP. DPc10 had no significant effect on the apparent affinity of the *L*-site or the maximum opening rate associated with this site (Fig. 7c; Table 1) suggesting that the effect of DPc10 is not due to alterations in luminal Ca^{2+} sensing mechanism.

The findings here with the DPc10 peptide basically fit with and considerably extend those found using mutated RyR2s. Specifically, as found here with DPc10, [^{3}H]ryanodine binding assays with RyR2s containing SCD mutations at residue 4496 in the C-domain exhibited slightly higher sensitivity to cytoplasmic Ca^{2+} and higher activity at sub-activating $[Ca^{2+}]_C$ than wild-type RyRs [c.f. Figs. 5a. 1a in (Jiang et al. 2002)]. That same study however could not resolve any significant difference between wild-type and mutant RyR2 in single channel measurements. This is not surprising, as the differences seen here in the Ca^{2+} activation properties of RyR2 in the presence and absence of DPc10 are quite small and would have been difficult to discern if the control and DPc10-induced activity had been determined in different channel populations, as was the case when comparing wild-type and mutant RyR2s (e.g. Jiang et al. 2002). Another striking similarity between the aberrant effects of SCD mutations and DPc10 is that they both cause a marked increase in the activation of RyRs by luminal Ca^{2+} (c.f. Fig. 7 and Jiang et al. 2004, 2005). The latter study (Jiang et al. 2005) shows that RyRs with the mutation R2474S (in the same region encompassed by DPc10) were at least tenfold more activated by luminal Ca^{2+} even though changes to cytoplasmic Ca^{2+} activation (mediated by the *A*-sites) were relatively small. We note that their experimental conditions favoured the flow of Ca^{2+} from the lumen to cytoplasm. This then is consistent with the results presented here which indicate that seemingly inconsequential changes to the *A*-sites, in conjunction with Ca^{2+} feed-through, can in fact lead to substantial changes in RyR2 activation by luminal Ca^{2+}. Therefore it is possible that much of the increased 'sensitivity' attributed solely to "luminal" effects of some SCD RyR2 mutations (Jiang et al. 2005) are due to changes in the cytoplasmic Ca^{2+} sites of the RyR.

A surprising finding was that DPc10 had no discernible effect on RyR2 activity in the presence of ATP. Unfortunately, the effects of the R2475S mutation in the presence of ATP have not yet been reported so that we cannot compare the peptide and the mutation under these conditions. These results do raise questions about the extent to which DPc10 mimics the functional outcomes of the R2475S mutation. Curiously, DPc10 added to more intact systems does, in fact, cause increased Ca^{2+} leak from the SR in the presence of ATP. This has been seen in Ca^{2+} release from isolated SR vesicles (Oda et al. 2005), and from the SR skinned- and intact cardiomyocytes (Oda et al. 2005; Yang et al. 2006). These findings suggest that the effects of DPc10 in vivo rely on key cellular components that are not present in the reduced bilayer system. One possibility is that DPc10 is somehow regulating the action of accessory proteins that modulate RyR2 activity in vivo that are absent in the bilayer studies. Although calsequestrin, triadin, junctin and FKBP12.6 are known to be present in the bilayer system (Ahern et al. 1997; Gyorke et al. 2004; Beard et al. 2005), calmodulin is likely to be absent because it dissociates in the high Ca^{2+} conditions needed for vesicle fusion (Balshaw et al. 2001). There are a number of accessory phosphatases and kinases known to regulate the activity of RyR2 in vivo (Marks 2001) whose presence in bilayer studies has not been determined. Another possibility is that the DPc10 effect in vivo is sensitive to post-translational modifications of RyR2 (e.g. oxidation, nitrosylation, phosphorylation) that are not controlled in the bilayer studies. For example, oxidative stress in failing hearts appears to unzip the central- and N-terminal domains and, in so doing, nullifies the action of DPc10 on RyR2 (Yano et al. 2005).

In this study, we explain how cytoplasmic perturbation of RyR2 can bestow increased channel sensitivity to luminal Ca^{2+}. CPVT and ARVD mutations cluster in regions of the RyR2 that are linked with cytoplasmic regulation of the channel (George et al. 2007) and we show that RyR2 sensitivity to cytoplasmic Ca^{2+} is increased by a peptide (DPc10) which is designed to disrupt cytoplasmic interdomain interactions, mimicking the action of SCD mutations. Moreover, DPc10 enhances RyR2 activation by

luminal Ca^{2+}. Whilst bilayer studies have clearly shown that both cytoplasmic and luminal Ca^{2+} sites contribute to channel activity, we show that DPc10 has no discernible effect on channel gating associated with the luminal sites. This study concludes that enhanced luminal activation of RyR2 by DPc10, and possibly SCD mutations in RyR2, are due to changes in the cytoplasmic Ca^{2+} activation site which sensitise the channel to feed-through of Ca^{2+} from the SR lumen.

Acknowledgments Thanks to Katherine Bradley, Paul Johnson and Bronwyn Hiles for assisting with the experiments. This work was supported by the National Health & Medical Research Council of Australia (Grant No. 234420), by the National Institute of health (NIH Grant No. 1 RO 1 HL072841) and by infrastructure grant from NSW Health through Hunter Medical Research Institute.

References

Ahern GP, Junankar PR, Dulhunty AF (1997) Subconductance states in single channel activity of skeletal muscle ryanodine receptors after removal of FKBP12. Biophys J 72:146–162

Balshaw DM, Xu L, Yamaguchi N, Pasek DA, Meissner G (2001) Calmodulin binding and inhibition of cardiac muscle calcium release channel (ryanodine receptor). J Biol Chem 276:20144–20153

Beard NA, Casarotto MG, Wei L, Varsanyi M, Laver DR, Dulhunty AF (2005) Regulation of ryanodine receptors by calsequestrin: effect of high luminal Ca^{2+} and phosphorylation. Biophys J 88:3444–3454

Bers DM (2001) Excitation–contraction coupling and cardiac contractile force. Kluwer, Dordrecht

Bers DM (2002a) Calcium and cardiac rhythms: physiological and pathophysiological. Circ Res 90:14–17

Bers DM (2002b) Cardiac excitation–contraction coupling. Nature 415:198–205

Brooks SP, Storey KB (1992) Bound and determined: a computer program for making buffers of defined ion concentrations. Anal Biochem 201:119–126

Cheng H, Lederer MR, Lederer WJ, Cannell MB (1996) Calcium sparks and $[Ca^{2+}]_i$ waves in cardiac myocytes. Am J Physiol 270:C148–159

George CH, Jundi H, Walters N, Thomas NL, West RR, Lai FA (2006) Arrhythmogenic mutation-linked defects in ryanodine receptor autoregulation reveal a novel mechanism of Ca^{2+} release channel dysfunction. Circ Res 98:88–97

George CH, Jundi H, Thomas NL, Fry DL, Lai FA (2007) Ryanodine receptors and ventricular arrhythmias: emerging trends in mutations, mechanisms and therapies. J Mol Cell Cardiol 42:34–50

Gyorke I, Gyorke S (1998) Regulation of the cardiac ryanodine receptor channel by luminal Ca^{2+} involves luminal Ca^{2+} sensing sites. Biophys J 75:2801–2810

Gyorke S, Gyorke I, Lukyanenko V, Terentyev D, Viatchenko-Karpinski S, Wiesner TF (2002) Regulation of sarcoplasmic reticulum calcium release by luminal calcium in cardiac muscle. Front Biosci 7:d1454–d1463

Gyorke I, Hester N, Jones LR, Gyorke S (2004) The role of calsequestrin, triadin, and junctin in conferring cardiac ryanodine receptor responsiveness to luminal calcium. Biophys J 86:2121–2128

Herrmann-Frank A, Lehmann-Horn F (1996) Regulation of the purified Ca^{2+}-release channel/ryanodine receptor complex of skeletal muscle sarcoplasmic reticulum by luminal calcium. Pflugers Arch 432:155–157

Ikemoto N, Yamamoto T (2002) Regulation of calcium release by interdomain interaction within ryanodine receptors. Front Biosci 7:d671–83

Jiang D, Xiao B, Zhang L, Chen SR (2002) Enhanced basal activity of a cardiac Ca^{2+} release channel (ryanodine receptor) mutant associated with ventricular tachycardia and sudden death. Circ Res 91:218–225

Jiang D, Xiao B, Yang D, Wang R, Choi P, Zhang L, Cheng H, Chen SR (2004) RyR2 mutations linked to ventricular tachycardia and sudden death reduce the threshold for store-overload-induced Ca^{2+} release (SOICR). Proc Natl Acad Sci USA 101:13062–13067

Jiang D, Wang R, Xiao B, Kong H, Hunt DJ, Choi P, Zhang L, Chen SR (2005) Enhanced store overload-induced Ca^{2+} release and channel sensitivity to luminal Ca^{2+} activation are common defects of RyR2 mutations linked to ventricular tachycardia and sudden death. Circ Res 97:1173–1181

Laver DR (2007) Ca^{2+} stores regulate ryanodine receptor Ca^{2+} release channels via luminal and cytosolic Ca^{2+} sites. Biophys J 92:3541–3555

Laver DR, Lamb GD (1998) Inactivation of Ca^{2+} release channels (ryanodine receptors RyR1 and RyR2) with rapid steps in $[Ca^{2+}]$ and voltage. Biophys J 74:2352–2364

Laver DR, Roden LD, Ahern GP, Eager KR, Junankar PR, Dulhunty AF (1995) Cytoplasmic Ca^{2+} inhibits the ryanodine receptor from cardiac muscle. J Memb Biol 147:7–22

Laver DR, O'Neill ER, Lamb GD (2004) Luminal Ca^{2+}-regulated Mg^{2+} inhibition of skeletal RyRs reconstituted as isolated channels or coupled clusters. J Gen Physiol 124:741–758

Lehnart SE, Wehrens XH, Marks AR (2005) Defective ryanodine receptor interdomain interactions may contribute to intracellular Ca^{2+} leak: a novel therapeutic target in heart failure. Circulation 111:3342–3346

Liu N, Colombi B, Memmi M, Zissimopoulos S, Rizzi N, Negri S, Imbriani M, Napolitano C, Lai FA, Priori SG (2006) Arrhythmogenesis in catecholaminergic polymorphic ventricular tachycardia: insights from a RyR2 R4496C knock-in mouse model. Circ Res 99:292–298

Lukyanenko V, Gyorke I, Gyorke S (1996) Regulation of calcium release by calcium inside the sarcoplasmic reticulum in ventricular myocytes. Pflugers Arch 432:1047–1054

Marks AR (2001) Ryanodine receptors/calcium release channels in heart failure and sudden cardiac death. J Mol Cell Cardiol 33:615–624

Marks PW, Maxfield FR (1991) Preparation of solutions with free calcium concentration in the nanomolar range using 1,2-bis(o-aminophenoxy)ethane-N,N,N′,N′-tetraacetic acid. Anal Biochem 193:61–71

Marks AR, Priori S, Memmi M, Kontula K, Laitinen PJ (2002) Involvement of the cardiac ryanodine receptor/calcium release channel in catecholaminergic polymorphic ventricular tachycardia. J Cell Physiol 190:1–6

McCarthy TV, Mackrill JJ (2004) Unravelling calcium-release channel gating: clues from a 'hot' disease. Biochem J 380:e1–e3

Oda T, Yano M, Yamamoto T, Tokuhisa T, Okuda S, Doi M, Ohkusa T, Ikeda Y, Kobayashi S, Ikemoto N, Matsuzaki M (2005) Defective regulation of interdomain interactions within the ryanodine receptor plays a key role in the pathogenesis of heart failure. Circulation 111:3400–3410

O'Neill ER, Sakowska MM, Laver DR (2003) Regulation of the calcium release channel from skeletal muscle by suramin and the

disulfonated stilbene derivatives DIDS, DBDS, and DNDS. Biophys J 84:1674–1689

Schlotthauer K, Bers DM (2000) Sarcoplasmic reticulum Ca^{2+} release causes myocyte depolarization. Underlying mechanism and threshold for triggered action potentials. Circ Res 87:774–780

Sitsapesan R, Williams AJ (1994a) Gating of the native and purified cardiac SR Ca^{2+}-release channels with monovalent cations as permeant species. Biophys J 67:1484–1494

Sitsapesan R, Williams AJ (1994b) Regulation of the gating of the sheep cardiac sarcoplasmic reticulum Ca^{2+}-release channel by luminal Ca^{2+}. J Memb Biol 137:215–226

Sitsapesan R, Williams AJ (1995) The gating of the sheep skeletal sarcoplasmic reticulum Ca^{2+}-release channel is regulated by luminal Ca^{2+}. J Memb Biol 146:133–144

Sitsapesan R, Williams AJ (1997) Regulation of current flow through ryanodine receptors by luminal Ca^{2+}. J Memb Biol 159:179–185

Stern MD (1992) Buffering of calcium in the vicinity of a channel pore. Cell Calcium 13:183–192

Thomas NL, George CH, Lai FA (2006) Role of ryanodine receptor mutations in cardiac pathology: more questions than answers? Biochem Soc Trans 34:913–918

Tiso N, Stephan DA, Nava A, Bagattin A, Devaney JM, Stanchi F, Larderet G, Brahmbhatt B, Brown K, Bauce B, Muriago M, Basso C, Thiene G, Danieli GA, Rampazzo A (2001) Identification of mutations in the cardiac ryanodine receptor gene in families affected with arrhythmogenic right ventricular cardiomyopathy type 2 (ARVD2). Hum Mol Genet 10:189–194

Tripathy A, Meissner G (1996) Sarcoplasmic reticulum lumenal Ca^{2+} has access to cytosolic activation and inactivation sites of skeletal muscle Ca^{2+} release channel. Biophys J 70:2600–2615

Wang R, Chen W, Cai S, Zhang J, Bolstad J, Wagenknecht T, Liu Z, Chen SR (2007) Localization of an NH(2)-terminal disease-causing mutation hot spot to the "clamp" region in the three-dimensional structure of the cardiac ryanodine receptor. J Biol Chem 282:17785–93

Xu L, Meissner G (1998) Regulation of cardiac muscle Ca^{2+} release channel by sarcoplasmic reticulum lumenal Ca^{2+}. Biophys J 75:2302–2312

Yamamoto T, Ikemoto N (2002) Peptide probe study of the critical regulatory domain of the cardiac ryanodine receptor. Biochem Biophys Res Commun 291:1102–1108

Yang Z, Ikemoto N, Lamb GD, Steele DS (2006) The RyR2 central domain peptide DPc10 lowers the threshold for spontaneous Ca^{2+} release in permeabilized myocytes. Circ Res 70:475–485

Yano M, Okuda S, Oda T, Tokuhisa T, Tateishi H, Mochizuki M, Noma T, Doi M, Kobayashi S, Yamamoto T, Ikeda Y, Ohkusa T, Ikemoto N, Matsuzaki M (2005) Correction of defective interdomain interaction within ryanodine receptor by antioxidant is a new therapeutic strategy against heart failure. Circulation 112:3633–43

Zahradnik I, Gyorke S, Zahradnikova A (2005) Calcium activation of ryanodine receptor channels-reconciling RyR gating models with tetrameric channel structure. J Gen Physiol 126:515–527